

Supplementary Information

Immunomodulatory lysophosphatidylserines are regulated by ABHD16A and ABHD12 interplay

Siddhesh S. Kamat^{1,2}, Kaddy Camara³, William H. Parsons^{1,2}, Dong-Hui Chen⁴, Melissa M. Dix^{1,2}, Thomas D. Bird^{4,5}, Amy R. Howell³, & Benjamin F. Cravatt^{1,2*}

¹Department of Chemical Physiology and ²The Skaggs Institute for Chemical Biology, The Scripps Research Institute, La Jolla, California.

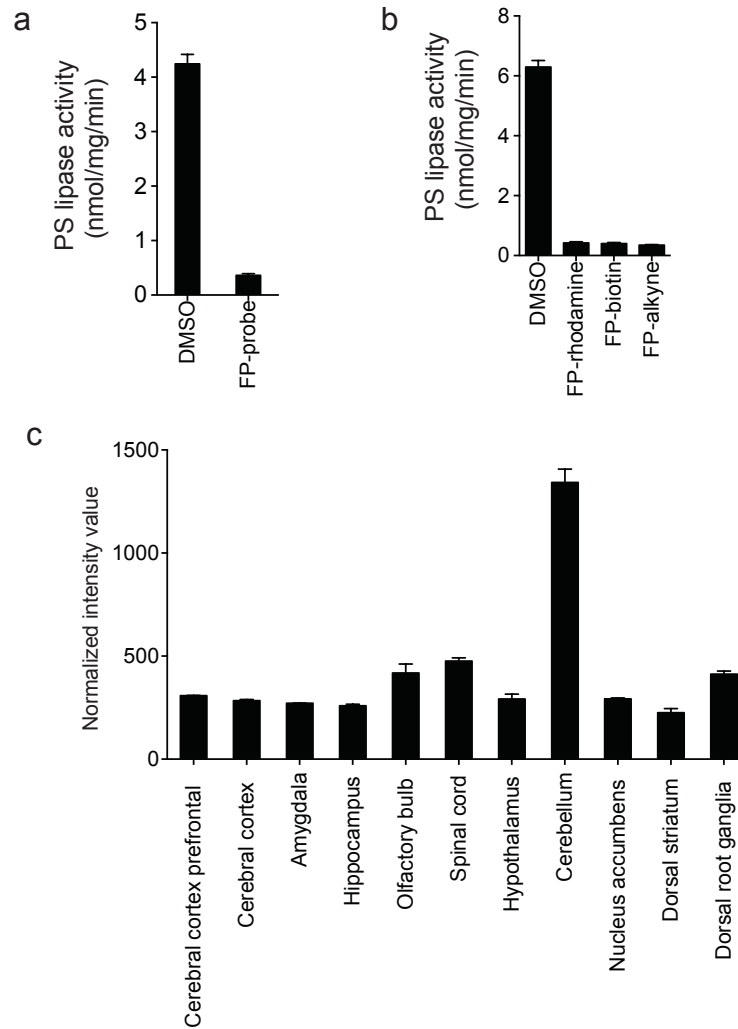
³Department of Chemistry, University of Connecticut, Storrs, Connecticut.

⁴Department of Neurology, University of Washington, Seattle, Washington.

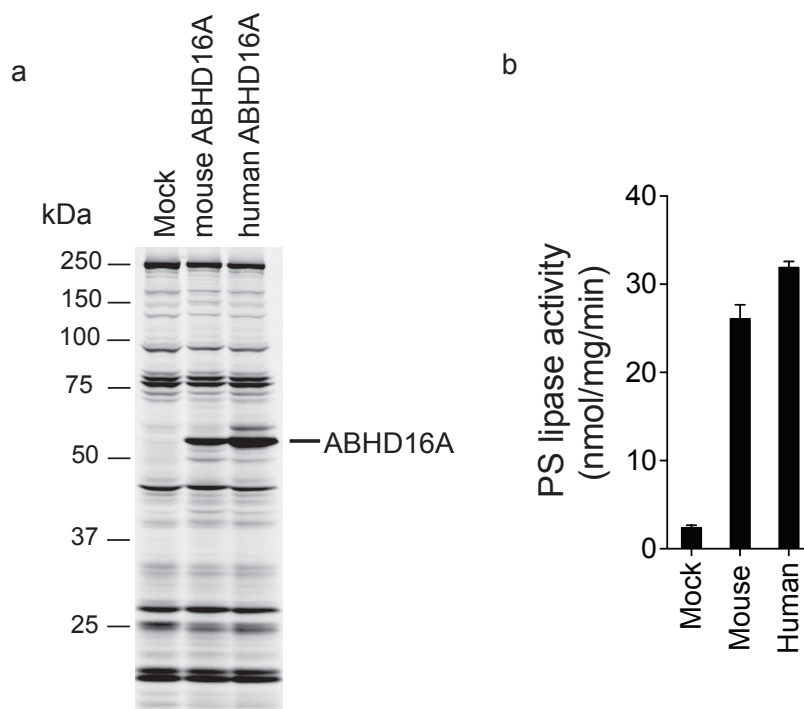
⁵Department of Medicine, University of Washington, Seattle, Washington.

*Email: cravatt@scripps.edu

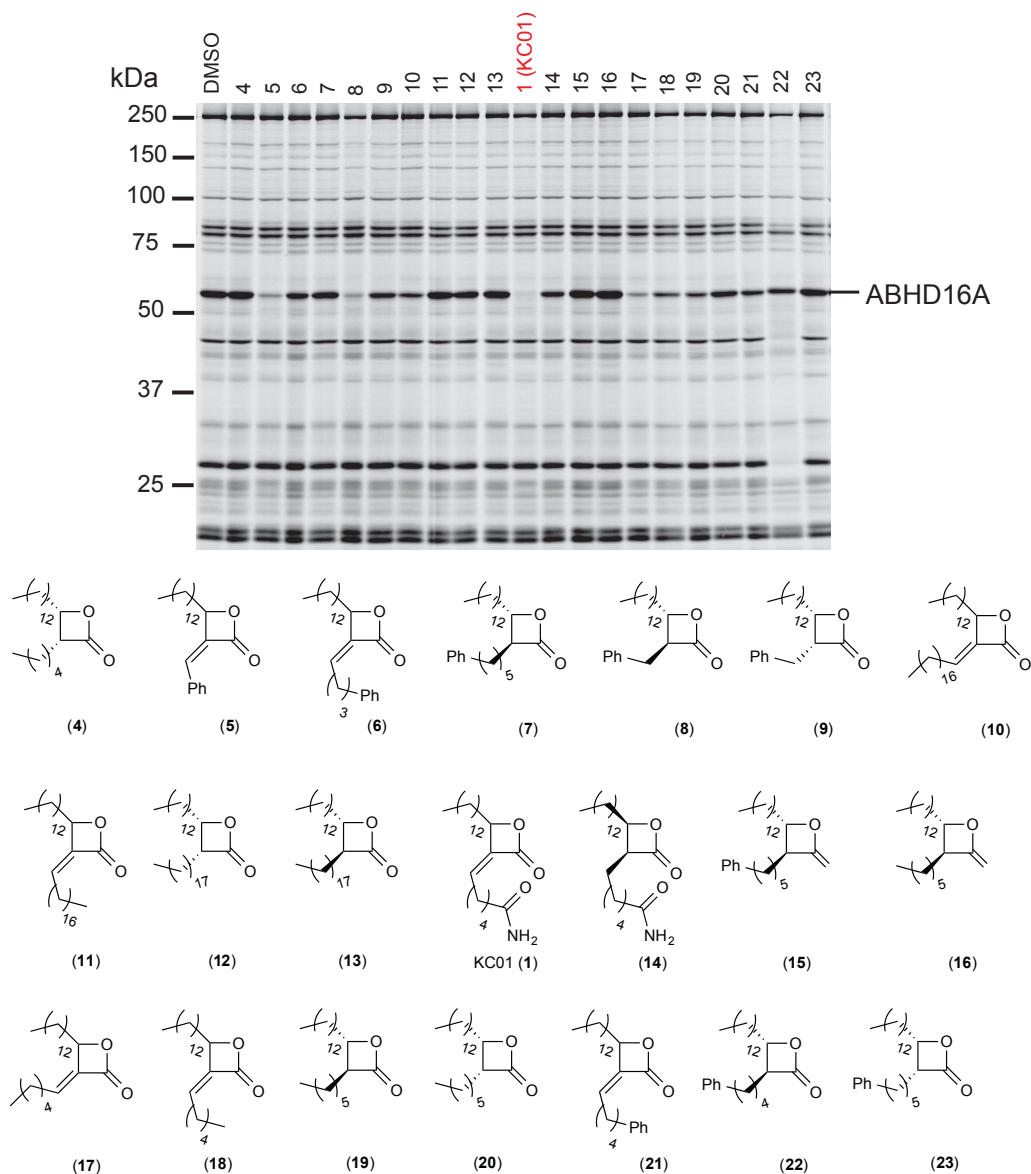
Supplementary Results



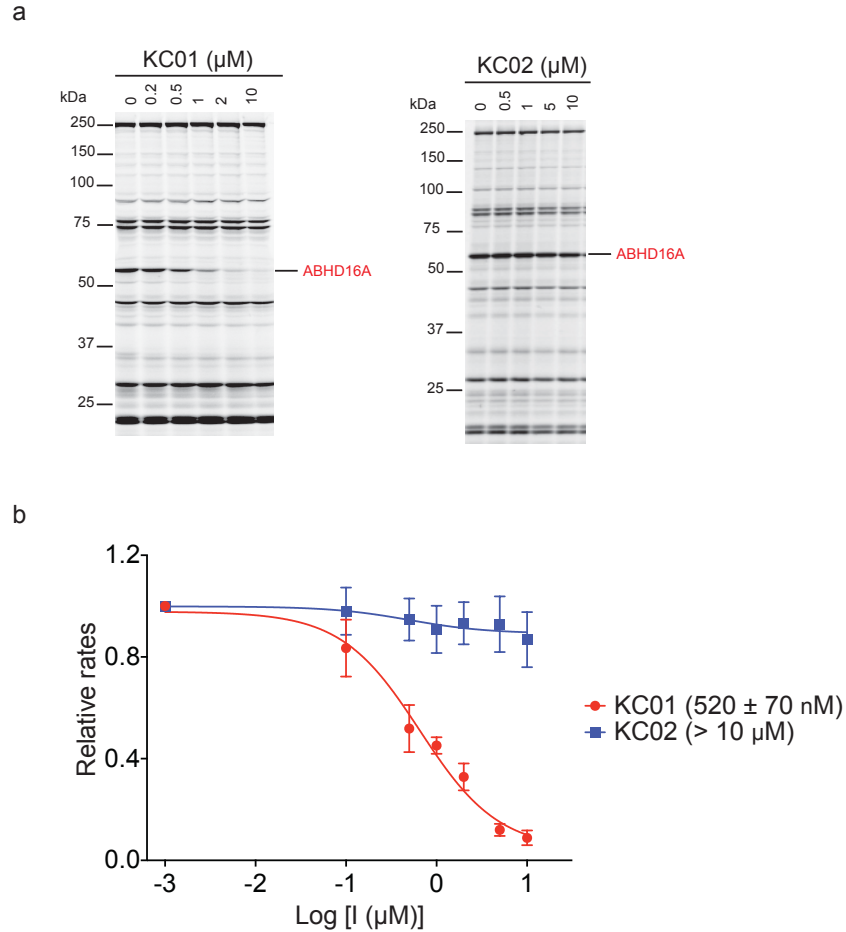
Supplementary Figure 1. Biochemical characterization of a PS lipase activity in mouse brain. (a) Mouse brain proteomes (1 mg/mL) were treated with DMSO or FP-rhodamine (FP-probe; 20 μ M, 30 min 37 $^{\circ}$ C) and then assayed for PS lipase activity with a C18:0/C18:2 PS substrate (100 μ M). Reactions were quenched and extracted with 2:1 CHCl_3 : CH_3OH , and the organic extracts analyzed by LC-MS as described in the **Supplementary Methods**. (b) Inhibition of mouse brain membrane fraction PS lipase activity by different FP-probes, assayed as described above. For (a) and (b), data represent mean values \pm s. e. m. for three biological replicates. (c) BioGPS gene expression profile for mouse *Abhd16a* in various regions of the brain and nervous system (<http://biogps.org/>).



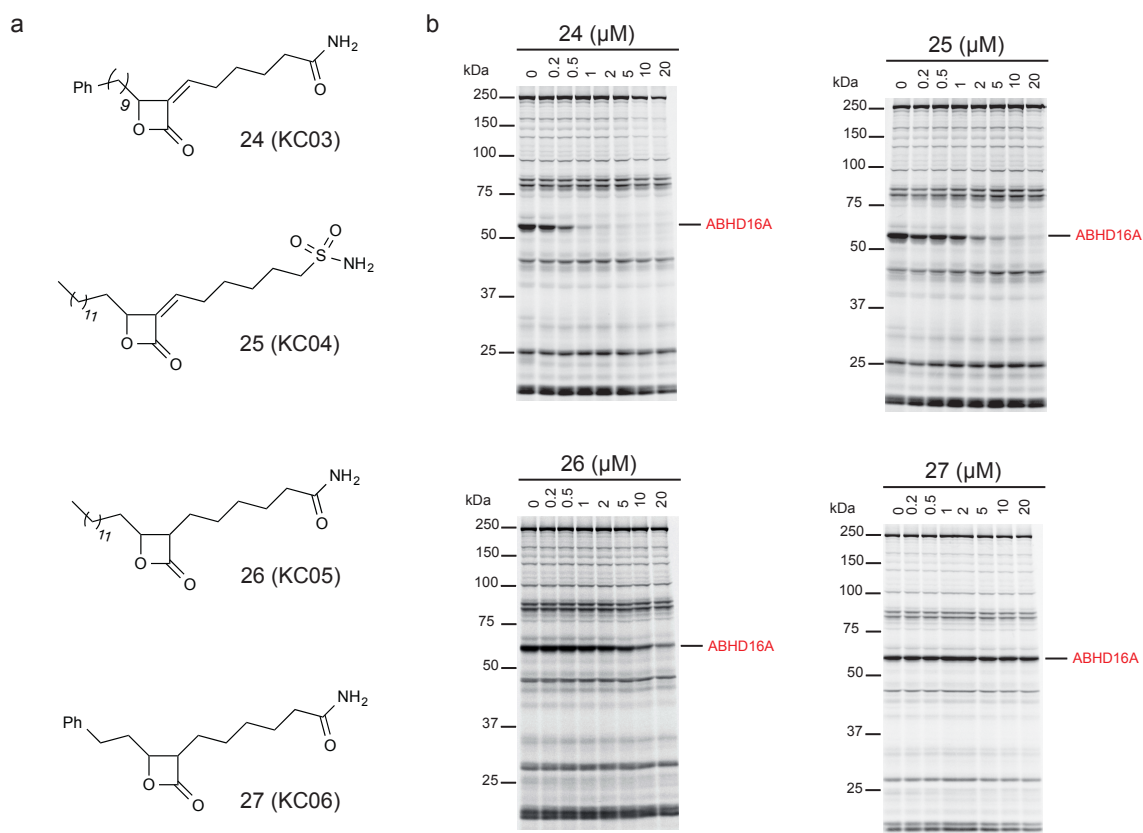
Supplementary Figure 2. Recombinant expression and activity of ABHD16A. (a) ABPP gel showing the expression and activity of mouse and human ABHD16A in transfected HEK293T cell proteomes compared to a mock-transfected HEK293T cell proteome. Gel-based ABPP experiments were performed by labeling 1 mg/mL of each proteome with FP-rhodamine (2 μ M, 30 min, 37 $^{\circ}$ C). Reactions were then quenched using SDS-PAGE loading buffer, separated by SDS-PAGE, and enzyme activities detected by in-gel fluorescence scanning (fluorescent gel shown in gray scale). Gel-based ABPP experiments were performed in triplicate with consistent results. (b) PS-lipase activity of mock-, mouse ABHD16A-, and human ABHD16A-transfected HEK293T membrane proteomes measured using a C18:0/C18:2 PS substrate (100 μ M). Assay was performed as described in **Supplementary Fig. 1**. Data represent mean values \pm s. e. m. for three biological replicates.



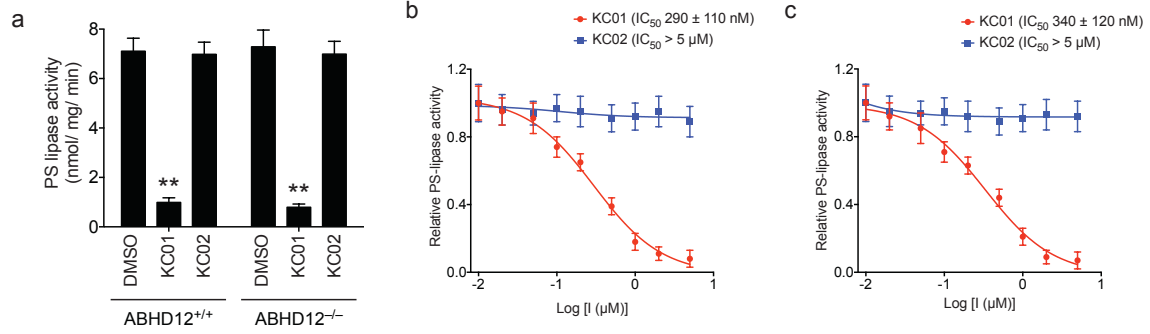
Supplementary Figure 3. Screening of α -alkylidene- β -lactones against human ABHD16A by competitive ABPP. Human ABHD16A-transfected HEK293T cell proteome (1 mg/mL) was pre-treated with α -alkylidene- β -lactones (10 μ M, 30 min, 37 $^{\circ}$ C) and then incubated with FP-rhodamine (2 μ M, 30 min, 37 $^{\circ}$ C), and the samples were analyzed by gel-based ABPP. Inhibitory activity was detected by loss of FP-rhodamine labeling of ABHD16A, and the selectivity of inhibitors was assessed by loss of other serine hydrolase activity signals detected by gel-based ABPP. Gel-based ABPP experiments were performed in duplicate with consistent results. The synthesis of α -alkylidene- β -lactones is provided either in the **Supplementary Methods** or in reference 1.



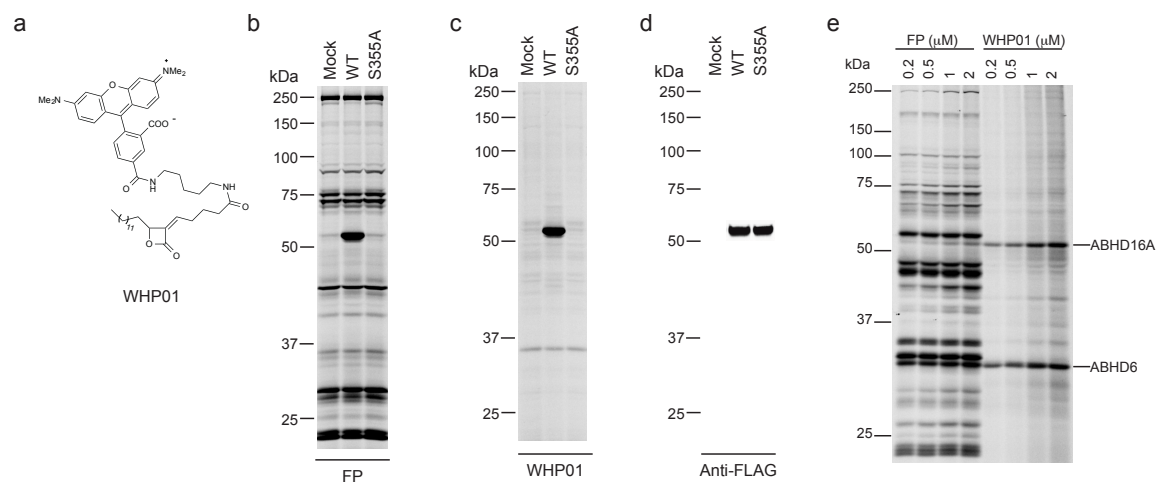
Supplementary Figure 4. Concentration-dependent inhibition of mouse ABHD16A activity. (a) The indicated concentrations of KC01 and KC02 were incubated with mouse ABHD16A-transfected HEK293T cell proteomes (1 mg/mL) for 30 min at 37 °C, and then samples were treated with FP-rhodamine (2 μM, 30 min, 37 °C), and analyzed by gel-based ABPP. From the data, an IC_{50} value of $\sim 0.5 \mu\text{M}$ was calculated for inhibition of mouse ABHD16A by KC01. KC02 did not inhibit mouse ABHD16A across the tested concentration range ($IC_{50} > 10 \mu\text{M}$). Gel-based ABPP experiments were performed in triplicate with consistent results. (b) Concentration dependent inhibition of the PS-lipase activity of mouse ABHD16A by KC01. Indicated concentrations of KC01 and KC02 were incubated with mouse ABHD16A-transfected HEK293T cell proteomes (30 min, 37 °C), and thereafter assayed using a C18:0/C18:2 PS substrate (100 μM). Assay was performed as described in **Supplementary Fig. 1**. The IC_{50} value obtained from this assay was $520 \pm 70 \text{ nM}$ for KC01. KC02 did not inhibit PS-lipase activity of mouse ABHD16A ($IC_{50} > 10 \mu\text{M}$). Data represent mean values \pm s. e. m. for three biological replicates.



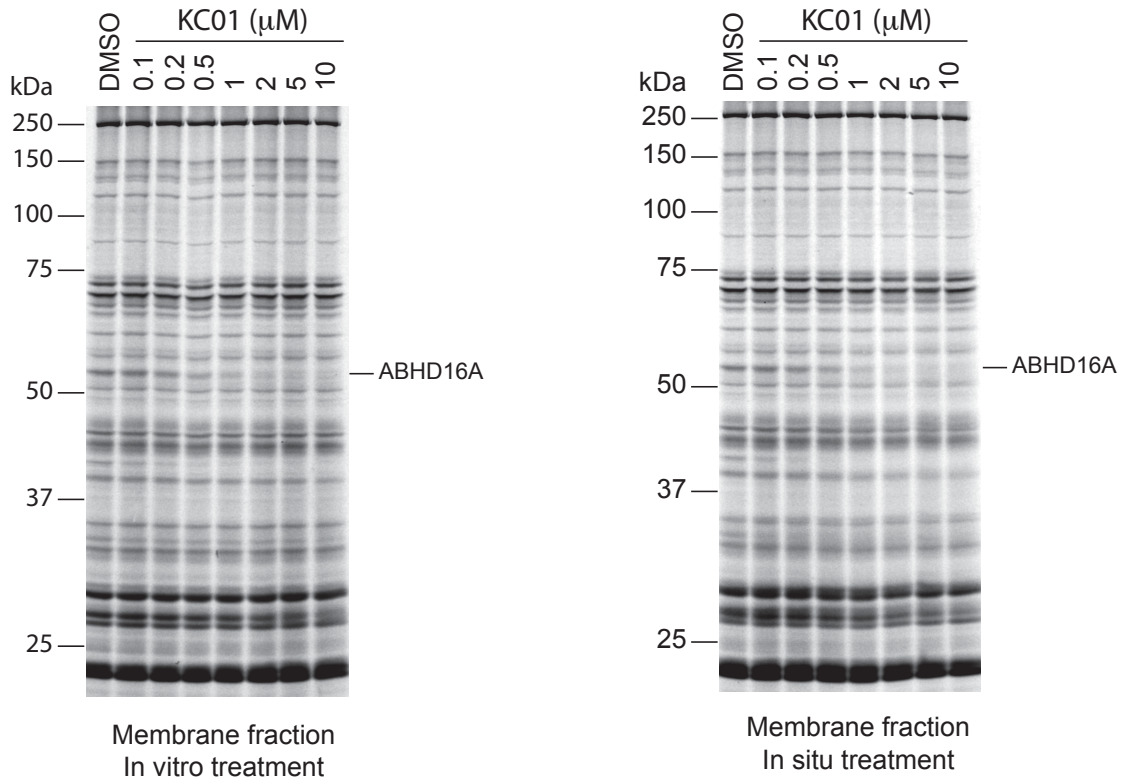
Supplementary Figure 5. Inhibitory activity of KC01 analogues against recombinant human ABHD16A as measured by competitive gel-based ABPP. (a) Structures of KC01 analogues. **(b)** Varying concentrations of the compounds were incubated with human ABHD16A-transfected HEK293T proteomes (1 mg/mL) for 30 min at 37 °C, and then samples were treated with FP-rhodamine (2 μM, 30 min, 37 °C), and analyzed by gel-based ABPP. From the data, the following IC_{50} values were estimated: **24** (KC03) (0.2 – 0.5 μM), **25** (KC04) (0.5 – 1 μM), **26** (KC05) (5 μM), and **27** (KC06) (> 20 μM) for ABHD16A. Gel-based ABPP experiments were performed in duplicate with consistent results.



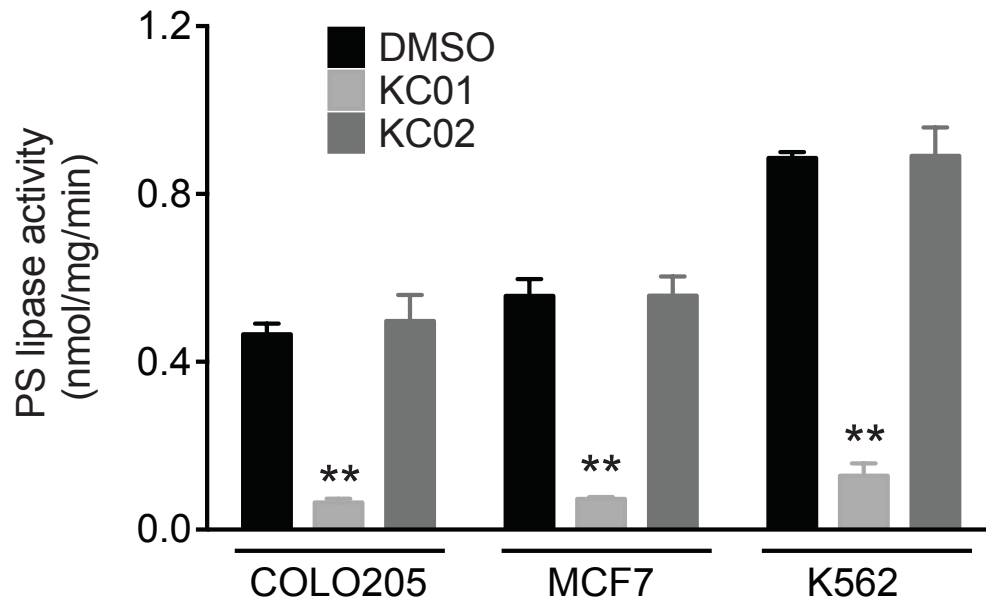
Supplementary Figure 6. Inhibition of PS lipase activity in mouse brain lysates from ABHD12^{+/+} and ABHD12^{-/-} mice. (a) PS lipase activity of mouse brain membrane lysates from ABHD12^{+/+} and ABHD12^{-/-} mice treated with KC01 or KC02 (1 μM, 30 min, 37 °C) and thereafter assayed using a C18:0/C18:2 PS substrate (100 μM). Data represent mean ± s. e. m. of three biological replicates. Student's t-test: ** p < 0.005 for KC01-treated versus DMSO-treated brain membrane lysates. Concentration-dependent inhibition of the PS lipase activities of brain membrane lysates from ABHD12^{+/+} (b) and ABHD12^{-/-} (c) mice. Indicated concentrations of KC01 and KC02 were incubated with brain membrane lysates (30 min, 37 °C) and thereafter assayed using a C18:0/C18:2 PS substrate (100 μM). Data represent mean values ± s. e. m. for three biological replicates.



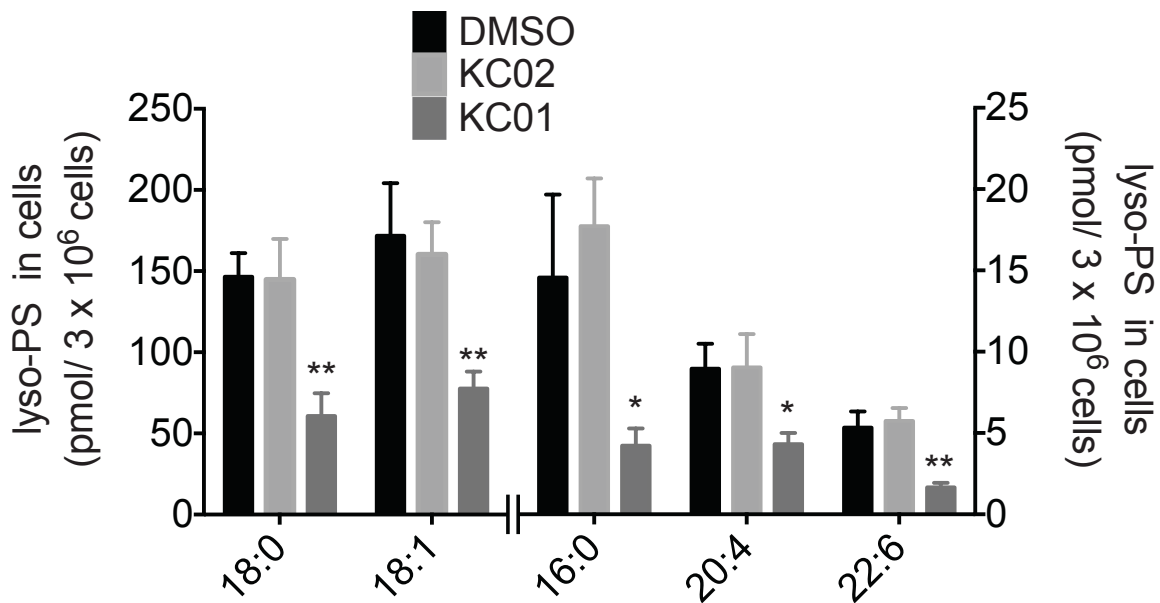
Supplementary Figure 7. Activity dependent labeling of ABHD16A by WHP01. (a) Structure of WHP01 (3), a fluorescent probe for ABHD16A. (b, c) ABPP gel of HEK293T cell lysates transfected with mock, wild type (WT)-ABHD16A (FLAG-tag) or a catalytic serine S355A-ABHD16A mutant (FLAG-tag) treated with (b) FP-rhodamine (2 μM, 30 min, 37 °C) or (c) WHP01 (0.2 μM, 30 min, 37 °C). (d) Western blot analysis (anti-FLAG) of the mock-, WT-ABHD16A-, and S355A-ABHD16A-transfected HEK293T lysates confirming the expression of WT- and S355A-ABHD16A in HEK293T cells. (e) Concentration-dependent labeling of endogenous ABHD16A in mouse brain membrane lysates by FP-rhodamine and WHP01 (30 min, 37 °C).



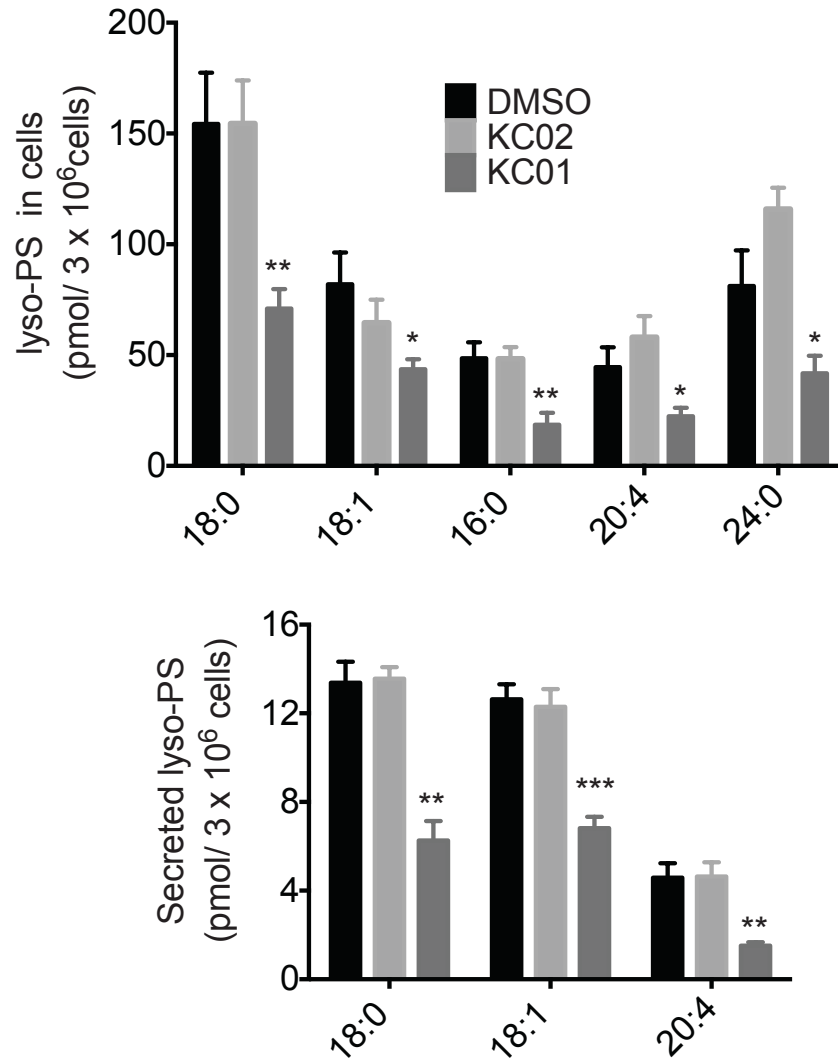
Supplementary Figure 8. Inhibitory activity of KC01 in the human K562 leukemia cell line as measured by competitive gel-based ABPP. The membrane proteome of K562 cells (left gel, *in vitro*) or cultured K562 cells (right gel, *in situ*) were treated with the indicated concentrations of KC01 (*in vitro*: 1 mg/mL proteome; 30 min treatment, 37 °C; *in situ*: 2 x 10⁶ cells; 4 h treatment, 37 °C), followed by FP-rhodamine (added *in vitro* to cell proteomes at 2 μM for 30 min, 37 °C) and analyzed by gel-based ABPP. Estimated *in vitro* and *in situ* IC₅₀ values for KC01 from the gel-based ABPP experiments were 0.2 – 0.5 μM. Gel-based ABPP experiments were performed in triplicate with consistent results.



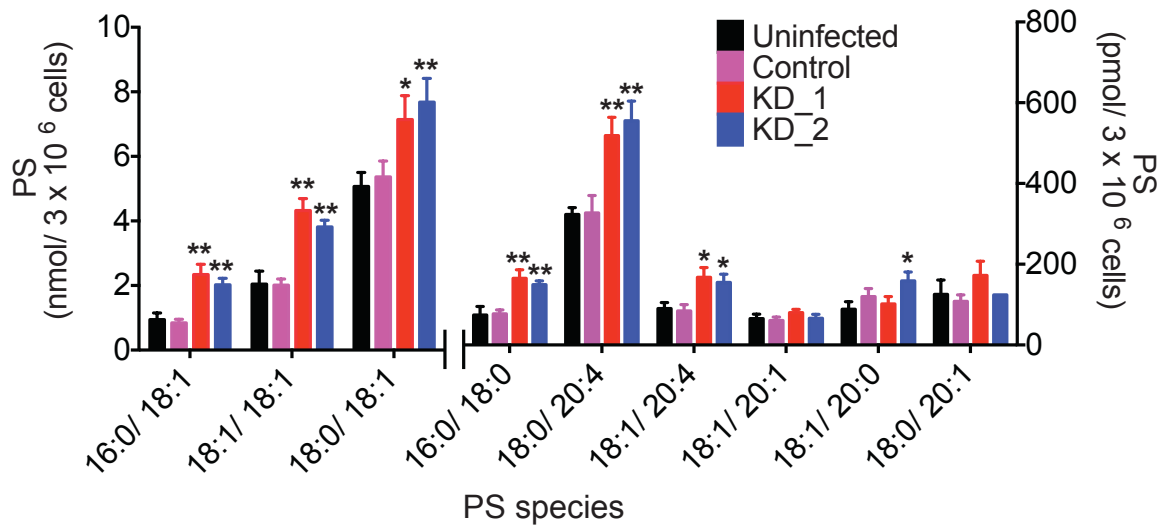
Supplementary Figure 9. The PS lipase activity of human cancer cells is blocked by KC01, but not KC02. The COLO205 (colon cancer), MCF7 (breast cancer) and K562 (leukemia) human cancer cell lines were treated *in situ* with inhibitors (KC01 or KC02, 1 μ M) or DMSO for 4 h. Cells were then harvested, lysed, and their membrane proteomes tested for PS-lipase activity using a C18:0/C18:2 PS substrate as described in **Supplementary Fig. 1**. For each cancer cell line, the PS-lipase activity was substantially decreased (> 90%) by KC01, but KC02 compared to DMSO controls. Data represent mean values \pm s. e. m for three biological replicates. Student's t-test: ** p < 0.005 for KC01-treated versus DMSO-treated cancer cells.



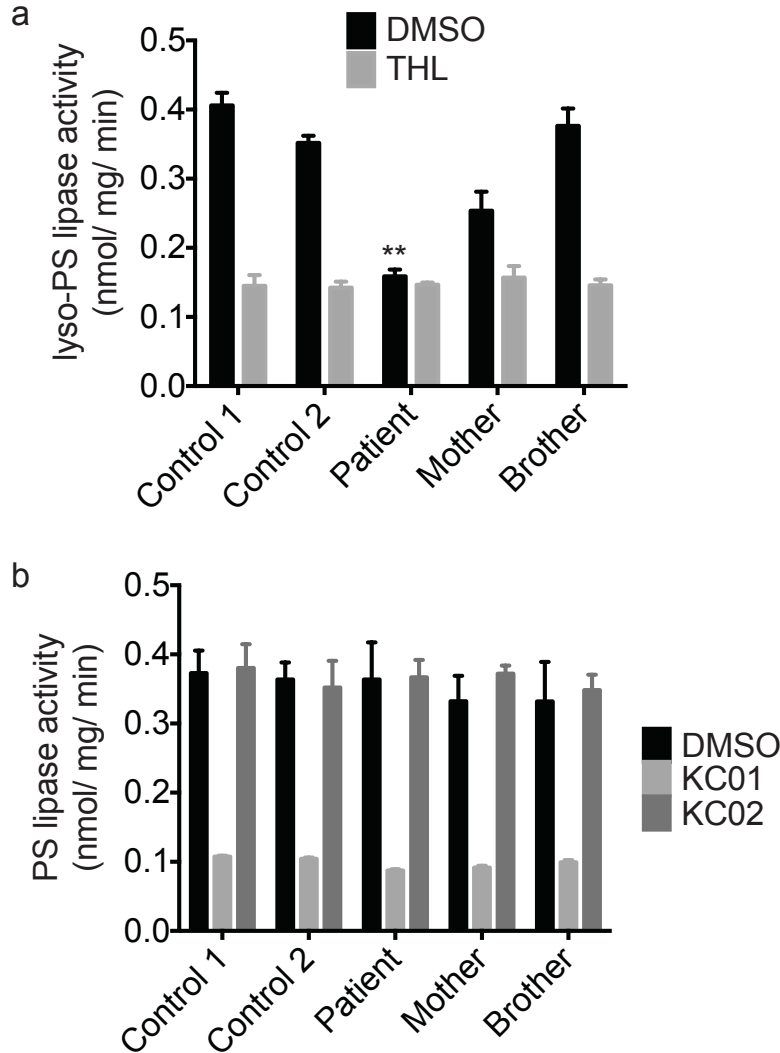
Supplementary Figure 10. Lyso-PS content of K562 cells treated with KC01 or KC02. K562 cells were treated with inhibitors (KC01 or KC02, 1 μ M) or DMSO for 4 h, and changes in cellular lyso-PS lipids were measured by targeted multiple reaction monitoring (MRM) methods as detailed in **Supplementary Methods**. Other lipid species were also quantified and are listed in **Supplementary Table 1**. Data represent mean values \pm s. e. m.; N = 8 per group. Student's t-test: * p < 0.05, ** p < 0.005 for KC01-treated versus DMSO-treated cells.



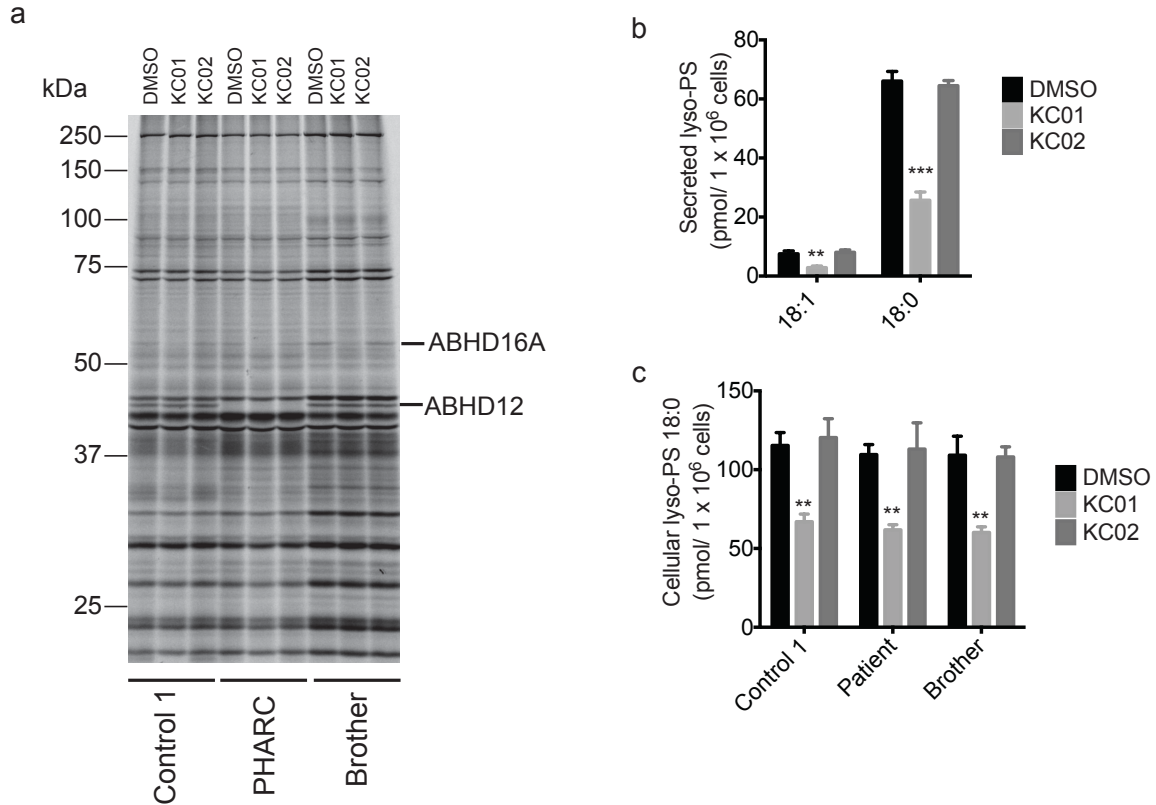
Supplementary Figure 11. Lyso-PS content of MCF7 cells treated with KC01 or KC02. MCF7 cells were treated with inhibitors (KC01 or KC02, 1 μ M) or DMSO for 4 h, and changes in cellular (upper graph) and secreted (lower graph) lyso-PS lipids were measured by targeted multiple reaction monitoring (MRM) methods as detailed in **Supplementary Methods**. Other lipid species were also quantified and are listed in **Supplementary Table 1**. Data represent mean values \pm s. e. m.; N = 8 per group. Student's t-test: * $p < 0.05$, ** $p < 0.005$, *** $p < 0.0001$ for KC01-treated versus DMSO-treated cells.



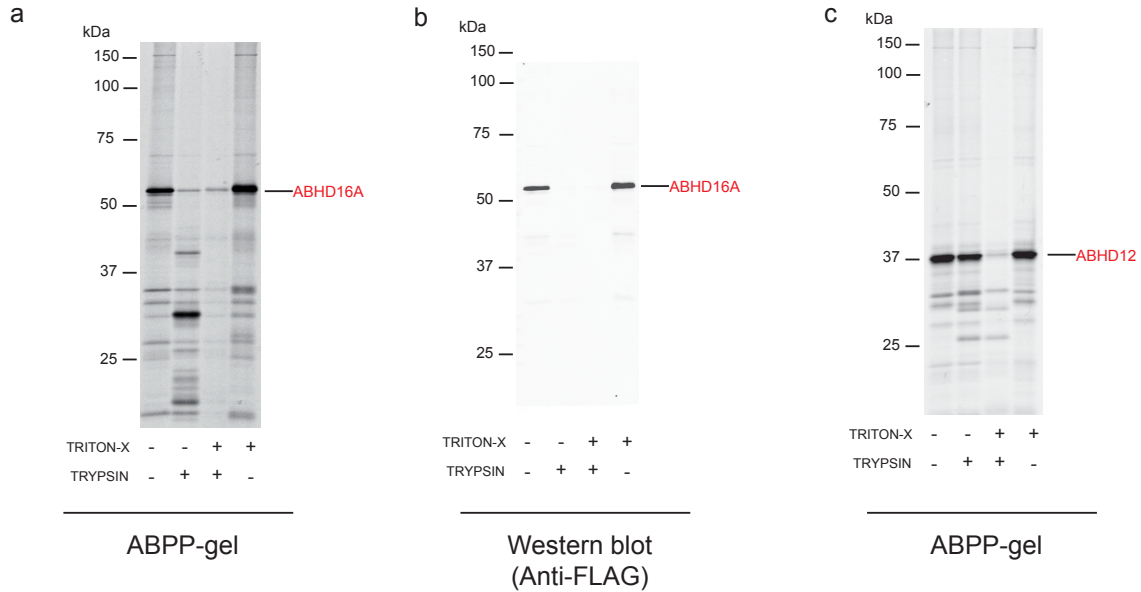
Supplementary Figure 12. PS content of K562 cells expressing different shRNA knockdown constructs. PS lipids were measured by targeted multiple reaction monitoring (MRM) methods as detailed in **Supplementary Methods**. Other lipid species were also quantified and are listed in **Supplementary Table 1**. Data represent mean values \pm s. e. m.; N = 8 per group. Student's t-test: * $p < 0.05$, ** $p < 0.005$ for KD_1 or KD_2 versus uninfected or control cells.



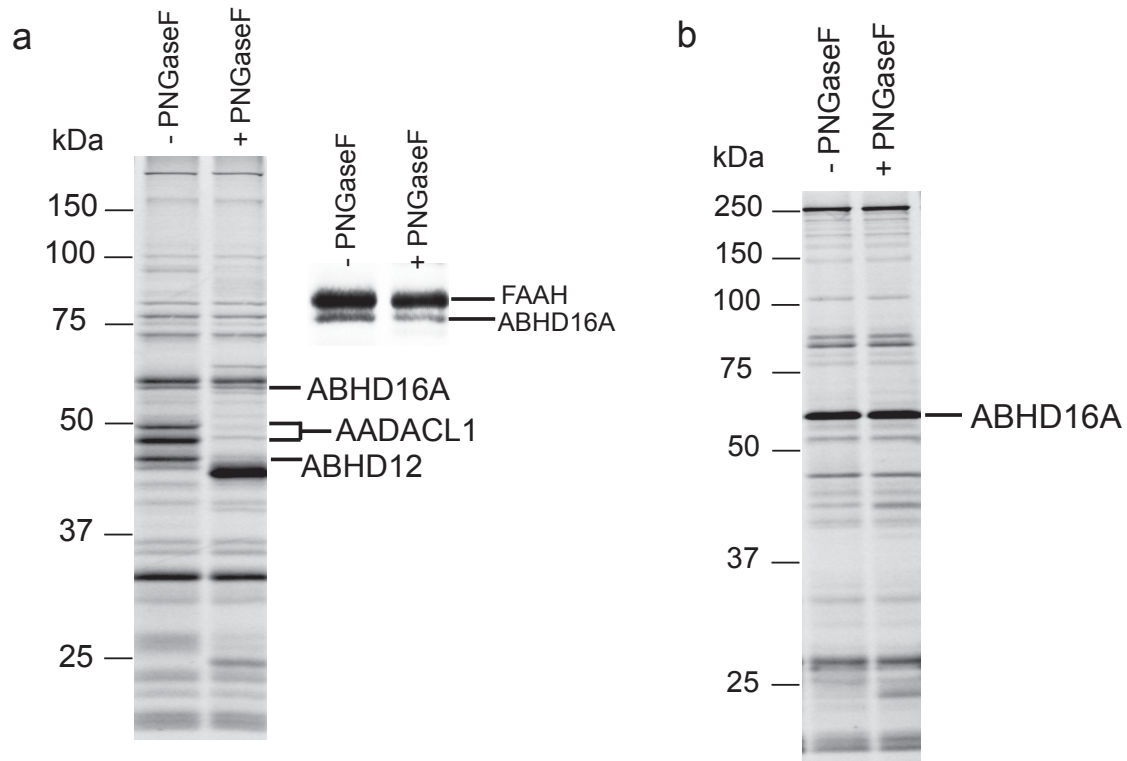
Supplementary Figure 13. Lyso-PS lipase and PS lipase activities of human lymphoblast cell lines (LCLs). (a) Lyso-PS lipase activity of membrane proteomes from indicated LCLs. Proteomes were pre-treated with DMSO or THL (10 μ M, 30 min, 37 $^{\circ}$ C) and then assayed for lyso-PS lipase activity using a C18:1 lyso-PS substrate (100 μ M) as described previously². (b) PS lipase activity of membrane proteomes from indicated LCLs. Proteomes were pre-treated with inhibitors (KC01 or KC02, 1 μ M) or DMSO for 30 min at 37 $^{\circ}$ C and then assayed for PS lipase activity using a C18:0/C18:2 PS substrate (100 μ M) as described in **Supplementary Fig. 1**. Note that KC01, but not KC02 substantially reduced the PS lipase activity of each LCL. Data represent mean values \pm s. e. m for three biological replicates. For part (a), Student's t-test: ** $p < 0.005$ for PHARC LCL versus Control 1 or Control 2 LCLs.



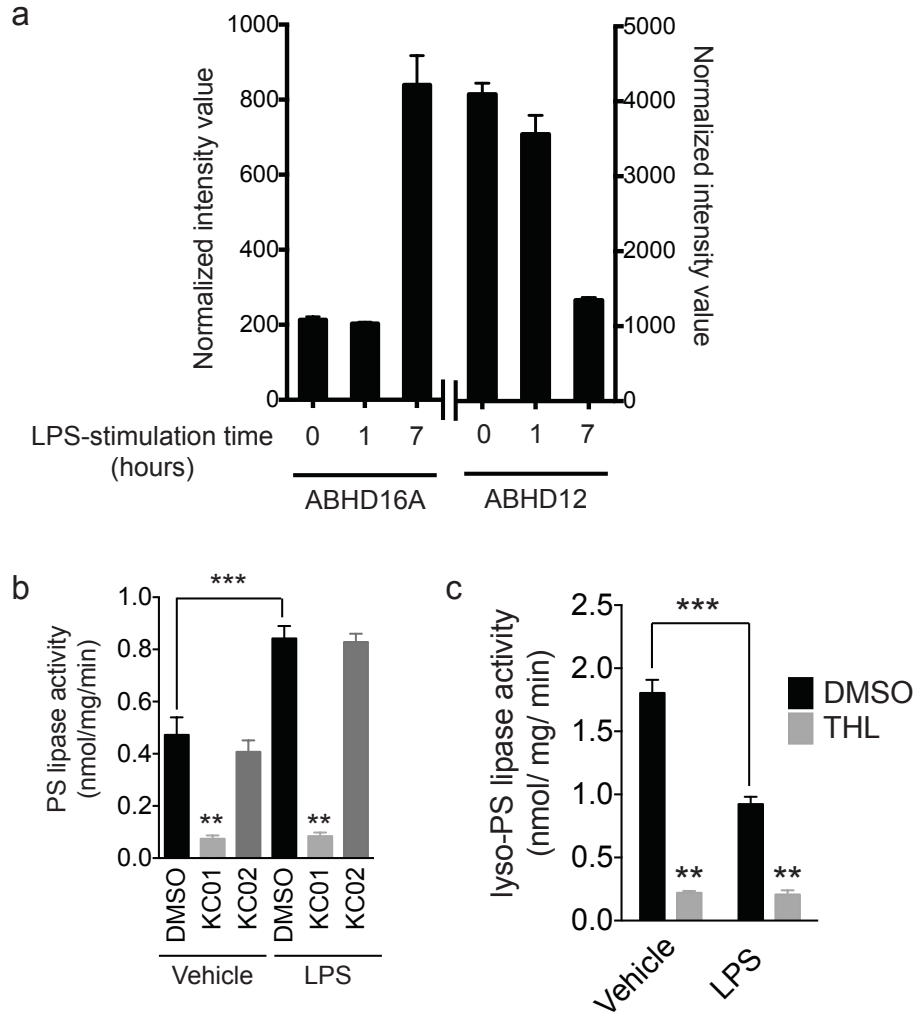
Supplementary Figure 14. Treatment of human LCLs with KC01 and KC02. (a) Gel-based ABPP analysis of the membrane proteome of indicated LCLs following treatment with inhibitors (KC01 or KC02, 1 μ M) or DMSO for 4 h (*in situ*). In addition to showing the selective loss of ABHD16A in KC01-treated cells, the ABPP gel also shows selective loss of ABHD12 in PHARC LCL compared to other LCLs. Gel-based ABPP experiments were performed in triplicate with consistent results. (b, c) Concentrations of secreted (b) and cellular (c) lyso-PS from PHARC LCL line (b) or PHARC and indicated Control lines (c) treated with inhibitors (KC01 or KC02, 1 μ M) or DMSO for 4 h. Other lipid species were also quantified and are listed in **Supplementary Table 1**. For (b, c), Data represent mean values \pm s. e. m. for four biological replicates. Student's t-test: ** $p < 0.005$, *** $p < 0.0001$ for KC01- versus DMSO-treated samples.



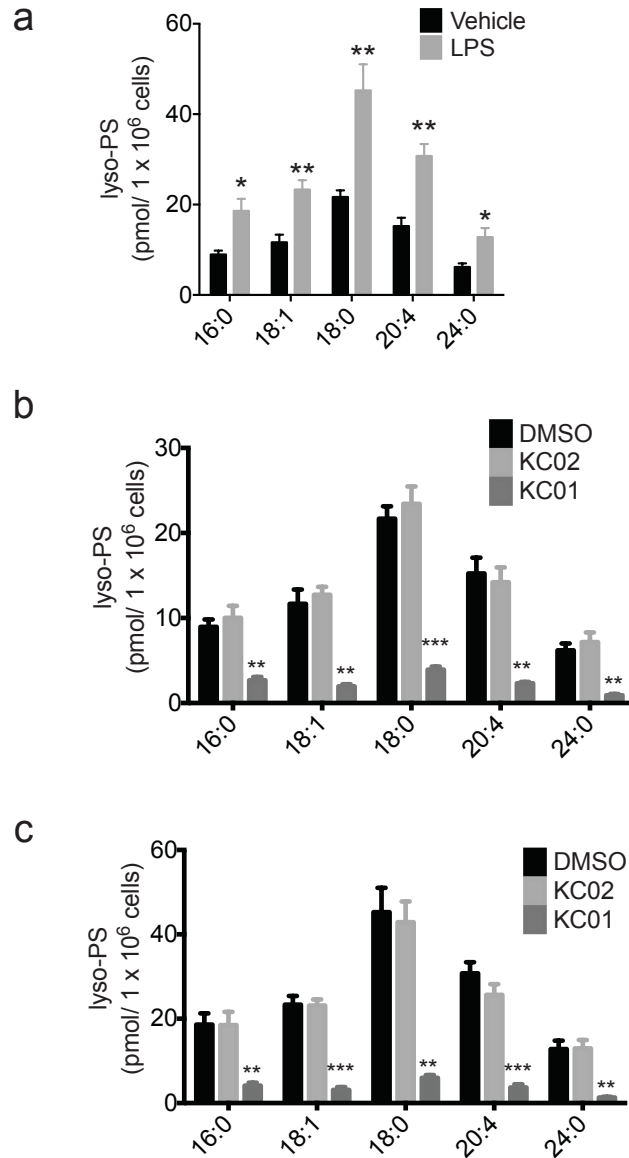
Supplementary Figure 15. Protease protection assays for ABHD16A and ABHD12. A C-terminal FLAG-tagged human ABHD16A construct was transfected into HEK293T cells, and the membrane proteome (1 mg/mL) of these cells was labeled with FP-rhodamine (2 μ M, 30 min, 37 $^{\circ}$ C) and treated with trypsin in the presence or absence of the detergent Triton-X. ABHD16A was susceptible to trypsin digestion with or without detergent as measured by gel-based ABPP (**a**) or anti-FLAG blotting (**b**), indicative of a cytosolically-oriented membrane protein. In contrast, ABHD12 only showed sensitivity to trypsin digestion in the presence of detergent (**c**), indicative of a lumenally-oriented membrane protein, as described previously³. Gel-based ABPP and western blotting experiments were performed in duplicate with consistent results.



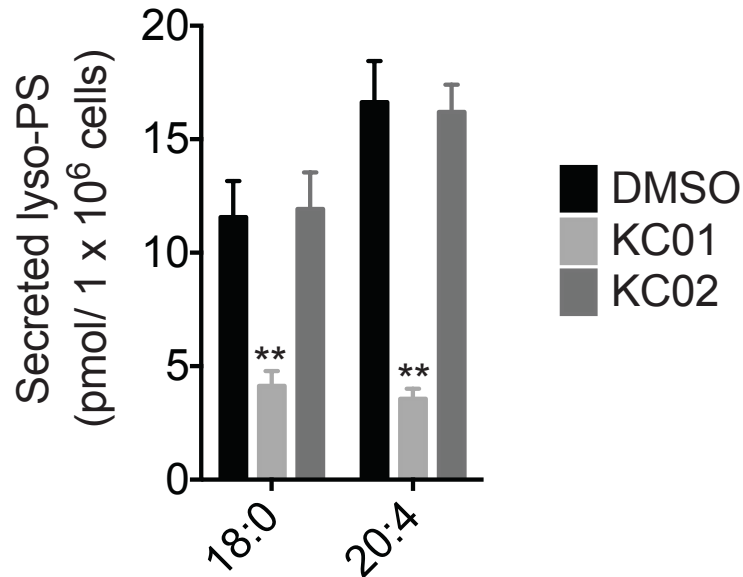
Supplementary Figure 16. Effect of PNGaseF treatment on SDS-PAGE migration of ABHD16A and ABHD12. (a, b) Mouse brain membrane proteome (1 mg/mL) (a) or ABHD16A-transfected HEK293T proteome (1 mg/mL) (b) was treated with FP-rhodamine (2 μ M, 30 min, 37 $^{\circ}$ C) and then exposed to PNGaseF. No change in the gel migration of endogenous brain (a, see inset) or recombinant (b) ABHD16A was observed in the presence of PNGaseF. In contrast, several other serine hydrolases showed changes in migration, including the lumenally oriented, glycoproteins AADAACL1 and ABHD12 (a). Gel-based ABPP experiments were performed in triplicate with consistent results.



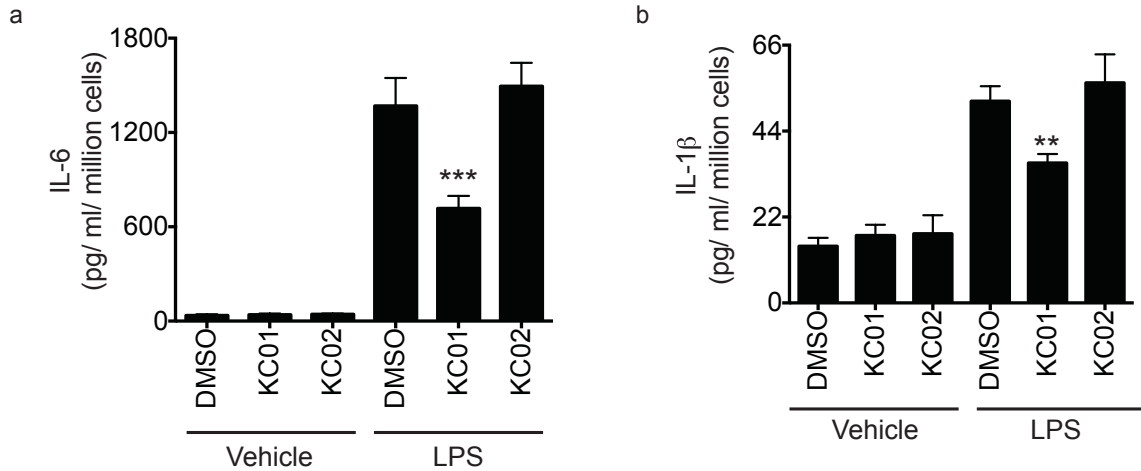
Supplementary Figure 17. Gene expression profile and activity of ABHD16A and ABHD12 in peritoneal macrophages. (a) BioGPS-derived gene expression profiles of ABHD16A and ABHD12 in mouse peritoneal macrophages following stimulation with lipopolysaccharide (LPS) for 0, 1, and 7 h. Original data can be found at: <http://biogps.org/>. (b) PS lipase activity of membrane proteomes of peritoneal macrophages treated with inhibitors (KC01 or KC02, 1 μ M) or DMSO for 30 min at 37 $^{\circ}$ C. Data represent mean values \pm s. e. m. for three biological replicates. (c) Lyso-PS lipase activity of membrane proteomes of peritoneal macrophages treated with DMSO, THL (10 μ M, 30 min 37 $^{\circ}$ C). For (b) and (c), vehicle- and LPS-treated macrophages were prepared as described in (a), and data represent mean values \pm s. e. m. for three biological replicates. Student's t-test: ** $p < 0.0005$ for KC01- versus DMSO-treated samples; *** $p < 0.0001$, for LPS- versus vehicle-treated samples.



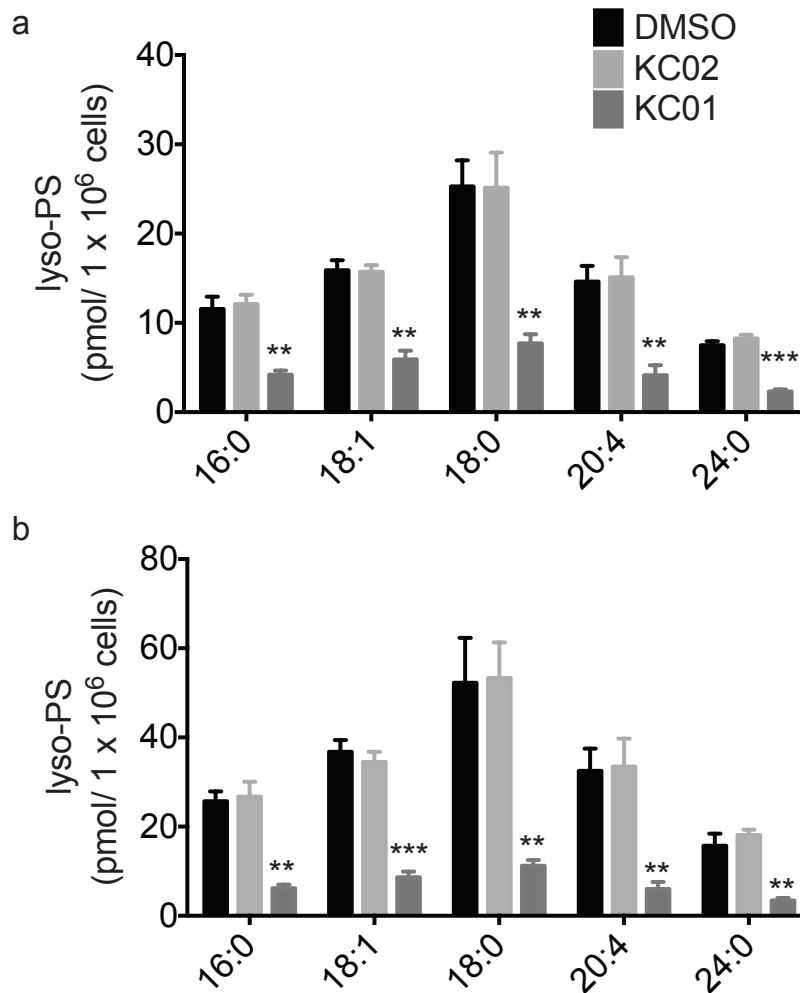
Supplementary Figure 18. Effect of LPS stimulation and KC01 and KC02 on cellular lyso-PS content of mouse macrophages. (a) Concentrations of cellular lyso-PS from thioglycollate-elicited peritoneal macrophages, treated with vehicle (PBS) or LPS (5 μ g/mL) for 7 h. Data represent mean values \pm s. e. m. for four biological replicates, Student's t-test: * $p < 0.05$, ** $p < 0.0005$ for LPS-treated versus vehicle-treated groups. (b, c) Concentration of cellular lyso-PS lipids from thioglycollate-elicited peritoneal mouse macrophages treated with inhibitors (KC01 or KC02, 1 μ M) or DMSO for 4 h, followed by stimulation with vehicle (PBS, a) or LPS (5 μ g/mL, b) for 7 h. All the other quantified lipid species are listed in **Supplementary Table 1**. Details for sample preparation and lipid measurements analysis can be found in **Supplementary Methods**. Data represent mean values \pm s. e. m. for four biological replicates. Student's t-test: ** $p < 0.005$, *** $p < 0.0001$ for KC01- versus DMSO-treated samples.



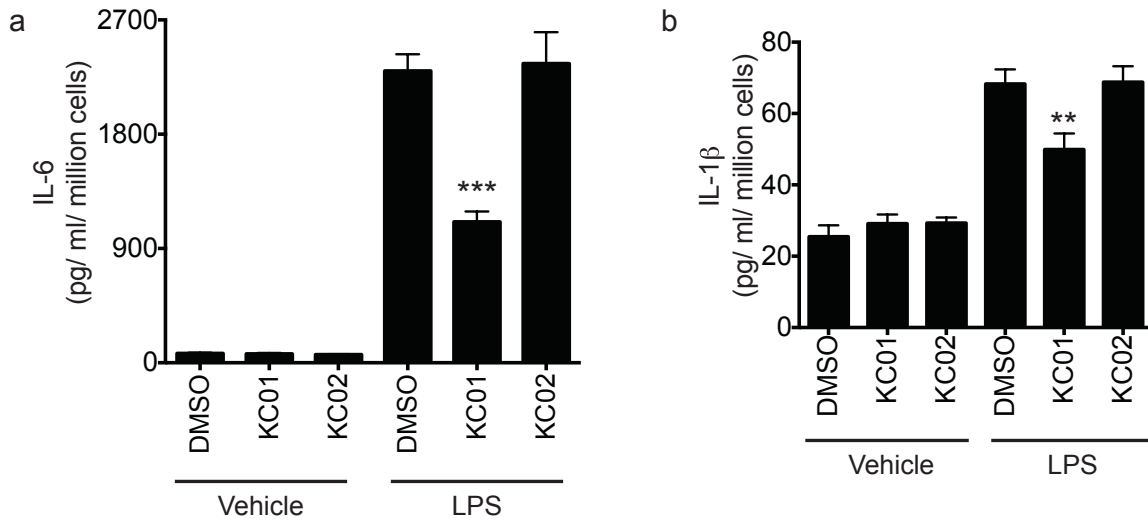
Supplementary Figure 19. Effect of KC01 and KC02 on secreted lyso-PS content of mouse macrophages. Concentration of secreted lyso-PS lipids from thioglycollate-elicited peritoneal mouse macrophages treated with inhibitors (KC01 or KC02, 1 μ M) or DMSO for 4 h, followed by treatment with PBS for 7 h (see **Fig. 4f** for a similar study performed on macrophages treated with LPS for 7 h). All the other quantified lipid species are listed in **Supplementary Table 1**. Details for sample preparation and lipid measurements analysis can be found in **Supplementary Methods**. Data represent mean values \pm s. e. m. for four biological replicates. Student's t-test: ** $p < 0.005$ for KC01- versus DMSO-treated samples.



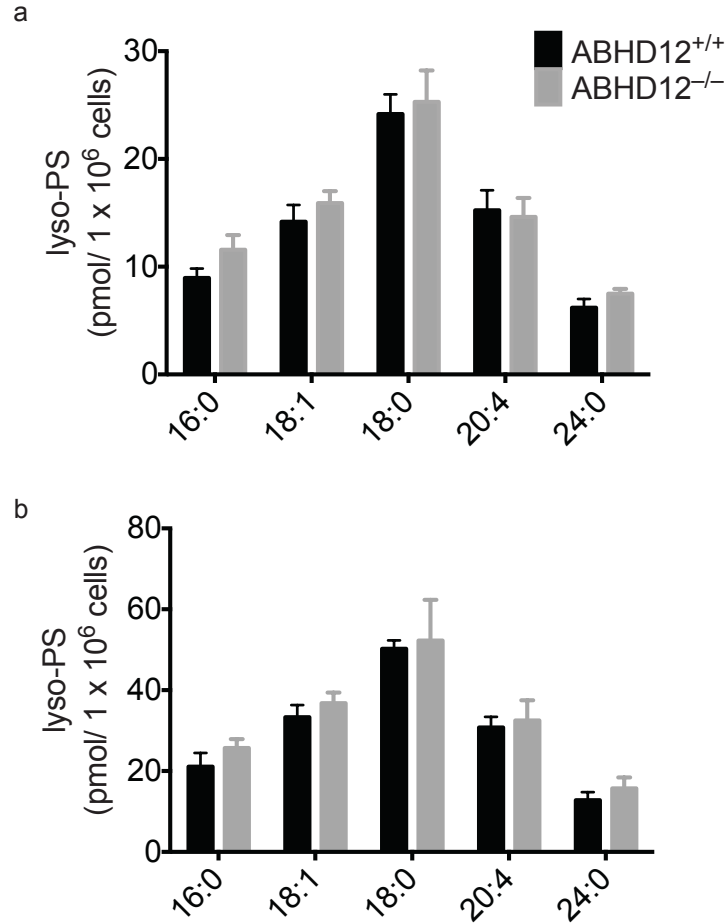
Supplementary Figure 20. Effect of KC01 and KC02 on secreted cytokines from mouse macrophages. Concentration of secreted cytokines from thioglycollate-elicited peritoneal mouse macrophages treated with inhibitors (KC01 or KC02, 1 μ M) or DMSO for 4 h followed by treatment with vehicle (PBS) or LPS (5 μ g/mL) for 7 h. Data represent mean values \pm s. e. m. for four biological replicates. Student's t-test: * $p < 0.05$, *** $p < 0.0001$ for KC01- versus DMSO-treated samples.



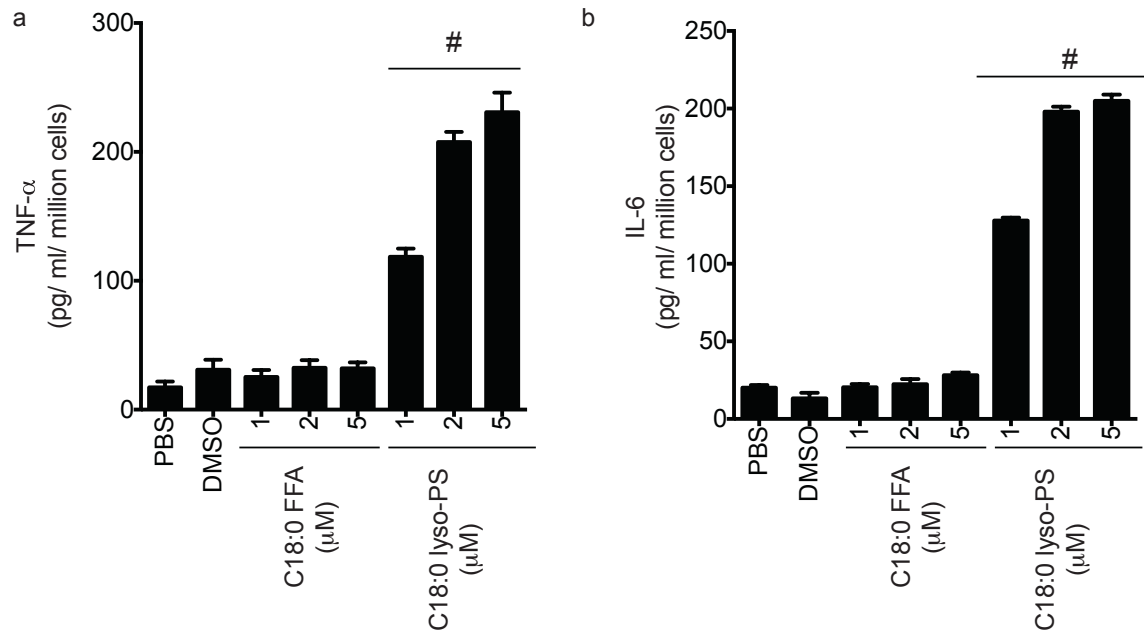
Supplementary Figure 21. Effect of KC01 and KC02 on cellular lyso-PS content of ABHD12^{-/-} macrophages. Concentration of cellular lyso-PS lipids from thioglycollate-elicited peritoneal mouse macrophages treated with inhibitors (KC01 or KC02, 1 μ M) or DMSO for 4 h, followed by stimulation with vehicle (PBS, **a**) or LPS (5 μ g/mL, **b**) for 7 h. All the other quantified lipid species are listed in **Supplementary Table 1**. Details for sample preparation and lipid measurements analysis can be found in **Supplementary Methods**. Data represent mean values \pm s. e. m. for four biological replicates. Student's t-test: ** $p < 0.005$, *** $p < 0.0001$ for KC01- versus DMSO-treated samples.



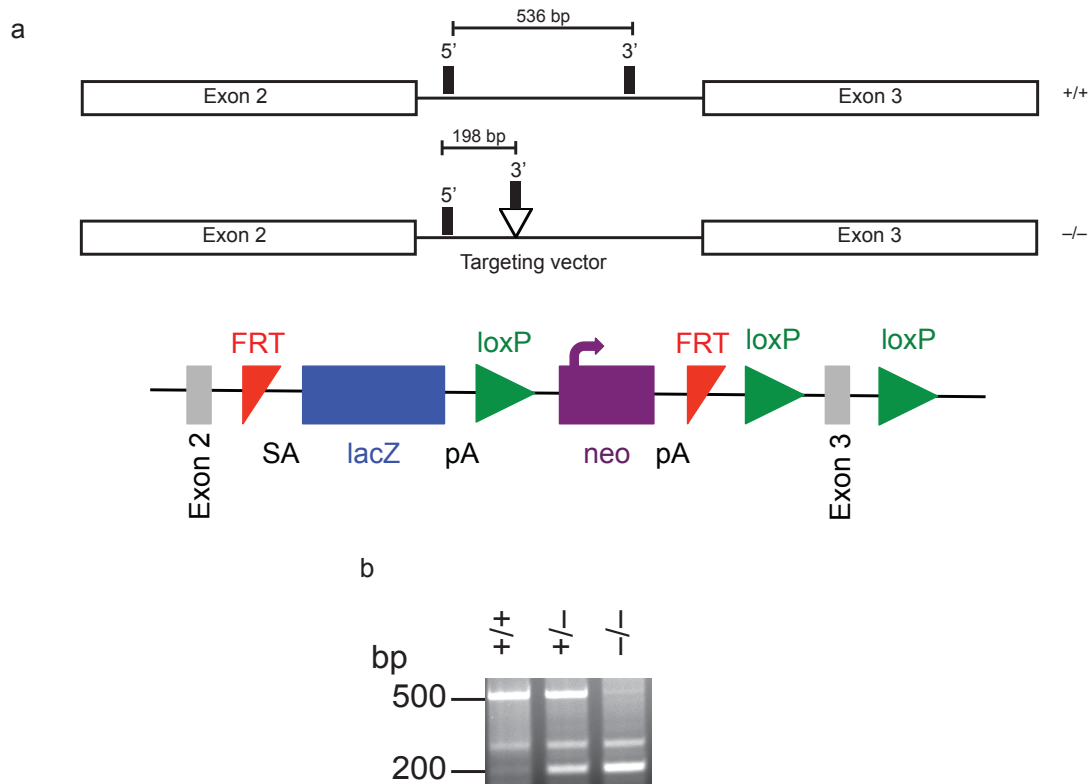
Supplementary Figure 22. Effect of KC01 and KC02 on secreted cytokines from ABHD12^{-/-} macrophages. Concentration of secreted cytokines from thioglycollate-elicited peritoneal mouse macrophages derived from ABHD12^{-/-} mice treated with inhibitors (KC01 or KC02, 1 μM) or DMSO for 4 h, followed by treatment with vehicle (PBS) or LPS (5 μg/mL) for 7 h. Data represent mean values ± s. e. m. for four biological replicates. Student's t-test: ** p < 0.005, *** p < 0.0001 for KC01- versus DMSO-treated samples.



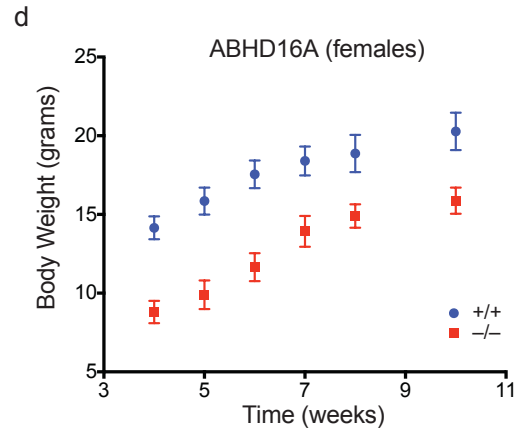
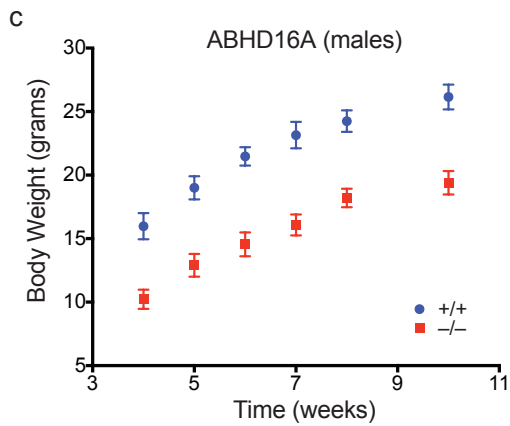
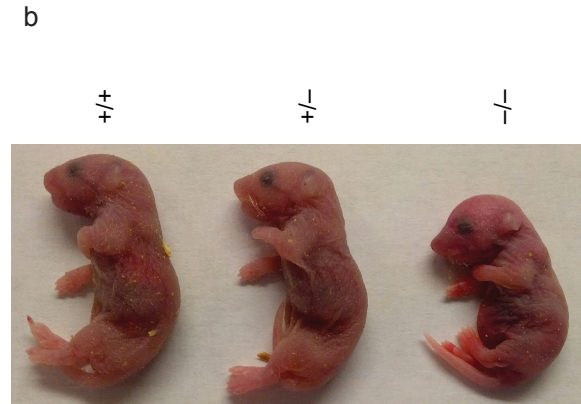
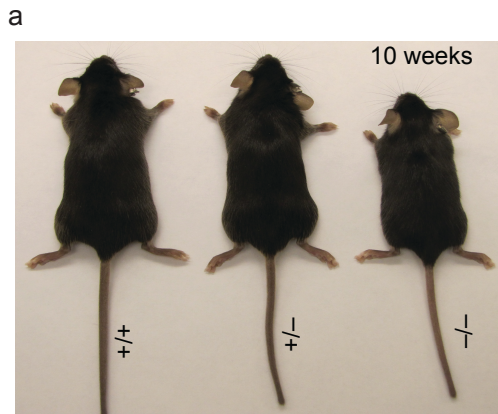
Supplementary Figure 23. Cellular lyso-PS content in ABHD12^{-/-} mouse peritoneal macrophages. The mouse thioglycollate-elicited peritoneal macrophages derived from ABHD12^{-/-} mice were treated with vehicle (PBS, **a**) or LPS (5 μ g/mL, **b**) for 7 hours. Thereafter changes in the cellular lyso-PS levels were measured by MRM methods. Details for the sample preparation and analysis can be found in **Supplementary Methods**. The cellular lyso-PS levels for both vehicle (**a**) and LPS-stimulated (**b**) macrophages were comparable to those observed for the ABHD12^{+/+} macrophages (**Fig. 4d**). All the other quantified lipid species are listed in **Supplementary Table 1**. Each group had four independent biological replicates and the bars represent data as mean \pm s. e. m.



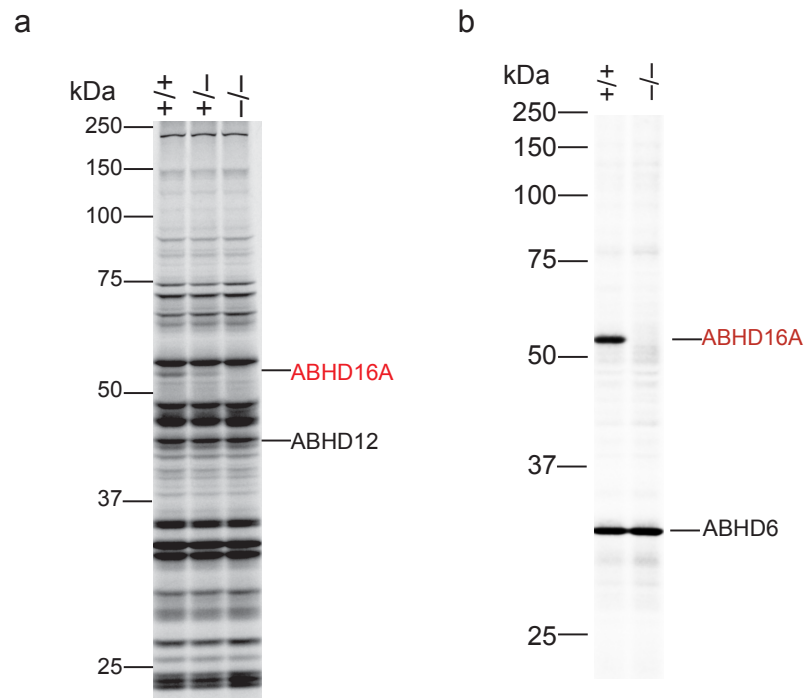
Supplementary Figure 24. Lyso-PS treatment promotes cytokine release from macrophages. Concentrations of secreted TNF- α (a) and IL-6 (b) from mouse peritoneal macrophages following treatment with DMSO or varying concentrations of C18:0 free fatty acid (FFA) or C18:0 lyso-PS (4 h treatment period). Treatments were performed in serum-free media. Data represent mean values \pm s. e. m. N = 8 per group. Student's t-test: # p < 0.0005 for C18:0 lyso-PS-versus DMSO-treated samples.



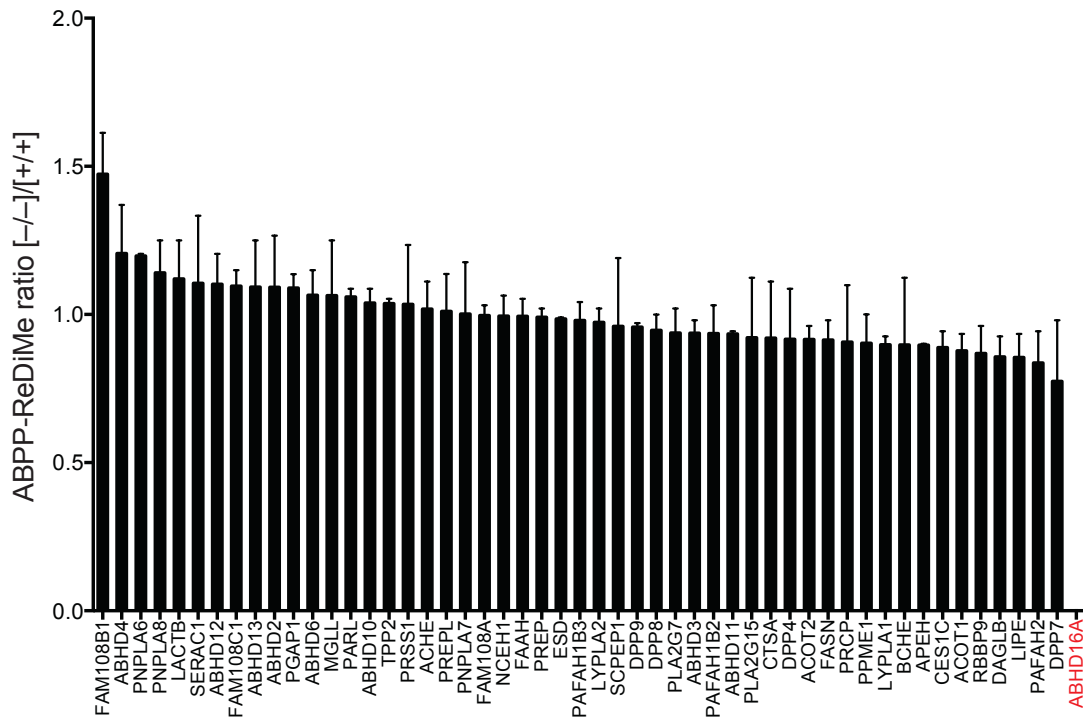
Supplementary Figure 25. Construct design and PCR genotyping for ABHD16A^{-/-} mice. (a) Schematic representation of the construct design for generation of the ABHD16A^{-/-} mice. The lower image shows the targeting construct design for the *Abhd16A* allele generated by Wellcome Trust Sanger Institute (http://www.mousephenotype.org/martsearch_ikmc_project/martsearch/ikmc_project/76829). Upper diagram shows expected PCR products for genotyping, where primers are located to generate 536 and 198 bp products for ABHD16A^{+/+} and ABHD16A^{-/-} genotypes, respectively. (b) A representative gel for the genotyping of ABHD16A mice is shown. Mouse tail genomic DNA was analyzed by standard PCR-based genotyping protocols. Homozygous ABHD16A^{+/+} mice show a single band of 536 bp, while homozygous ABHD16A^{-/-} mice show a single band at 198 bp. These PCR fragment sizes match those expected for the construct design (a).



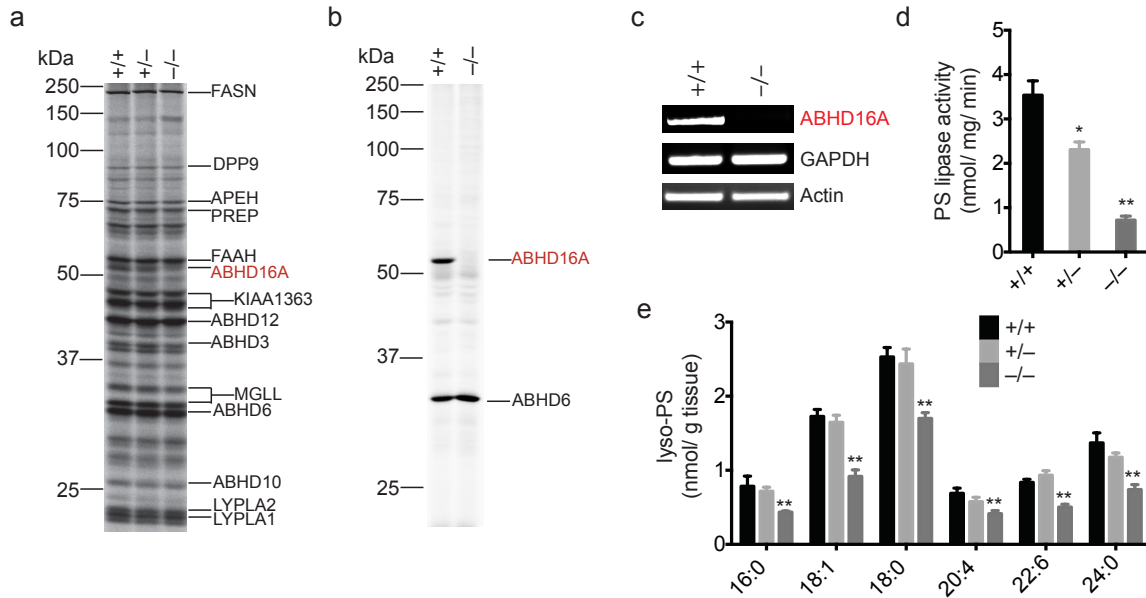
Supplementary Figure 26. Reduced size of ABHD16A^{-/-} mice. (a, b) Pictures of ABHD16A^{+/+}, ABHD16A^{+/-}, and ABHD16A^{-/-} littermate male mice at 10 weeks (a) and 1-day (b) of age showing smaller size of ABHD16A^{-/-} animals. (c, d) Body weights of the ABHD16A^{+/+} and ABHD16A^{-/-} male (c) and female (d) mice recorded from weaning (four weeks) until 10 weeks of age. Data represent mean \pm s. e. m. N = 4 per group.



Supplementary Figure 27. Serine hydrolase activity profile for whole brain proteomes of ABHD16A^{+/+}, ^{+/-}, and ^{-/-} mice. ABPP analysis of whole brain membrane proteomes from ABHD16A^{+/+}, ^{+/-}, and ^{-/-} mice treated with (a) FP-rhodamine (2 μ M, 30 min, 37 $^{\circ}$ C) or (b) WHP01 (0.5 μ M, 30 min, 37 $^{\circ}$ C) confirms complete and selective loss of ABHD16A in the ABHD16A^{-/-} mice.

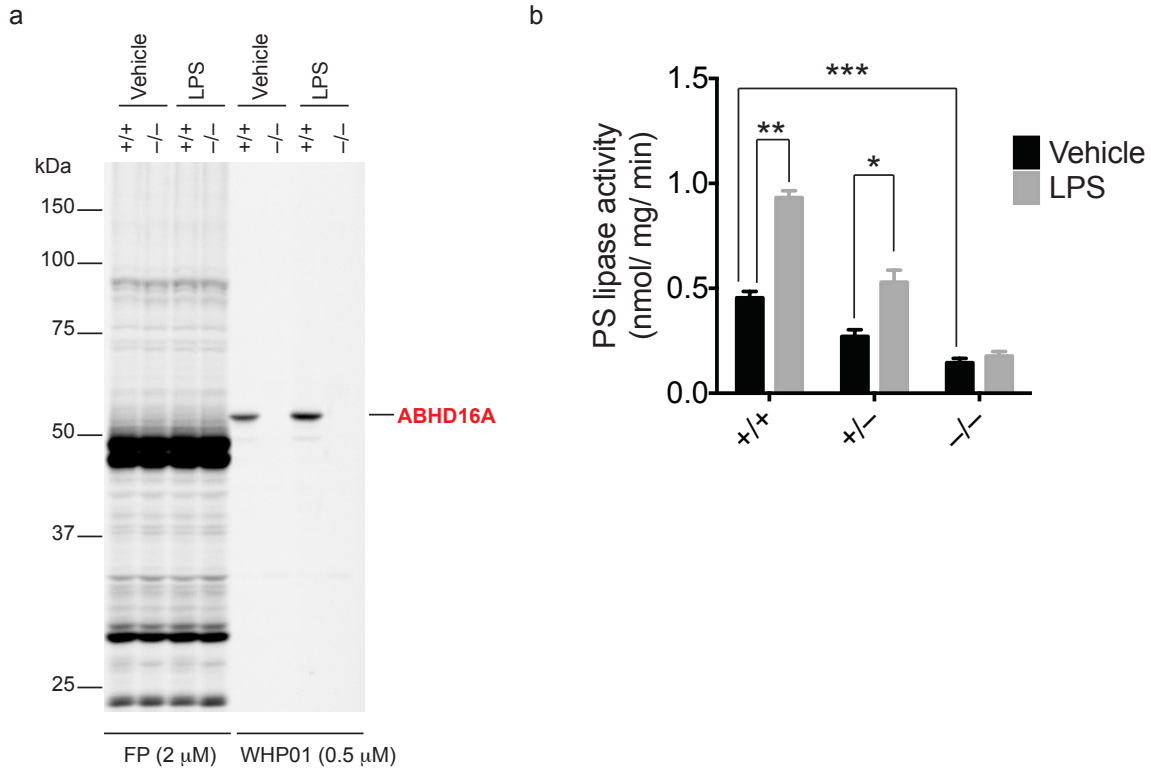


Supplementary Figure 28. Quantitative MS-based ABPP confirms loss of ABHD16A in brain tissue from ABHD16A^{-/-} mice. Serine hydrolase activities were measured by an ABPP-quantitative MS-based proteomic method involving reductive dimethylation (ReDiMe) of tryptic peptides with heavy and light formaldehyde (See **Supplementary Methods** for more details). Data represent average median ratios \pm s. d. for all quantified tryptic peptides per enzyme from two biological replicates.

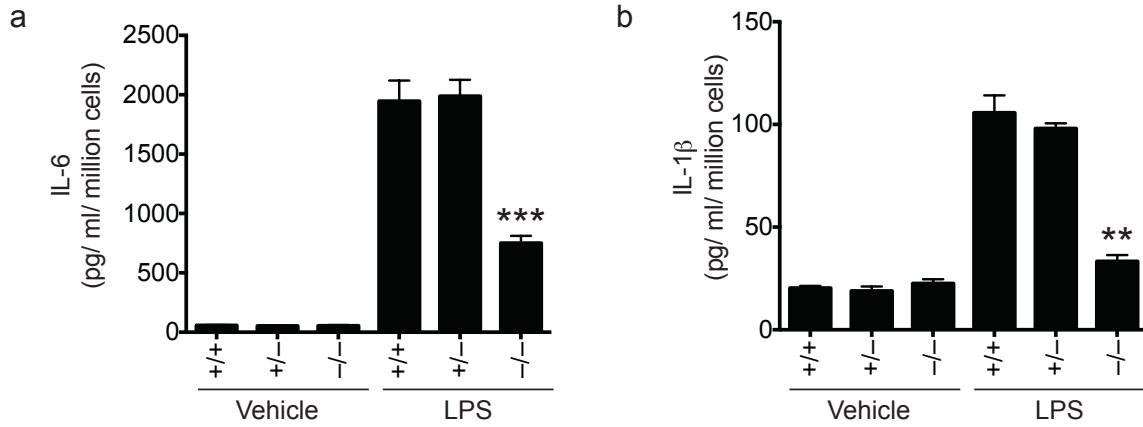


Supplementary Figure 29. Analysis of spinal cord tissue of ABHD16A^{-/-} mice.

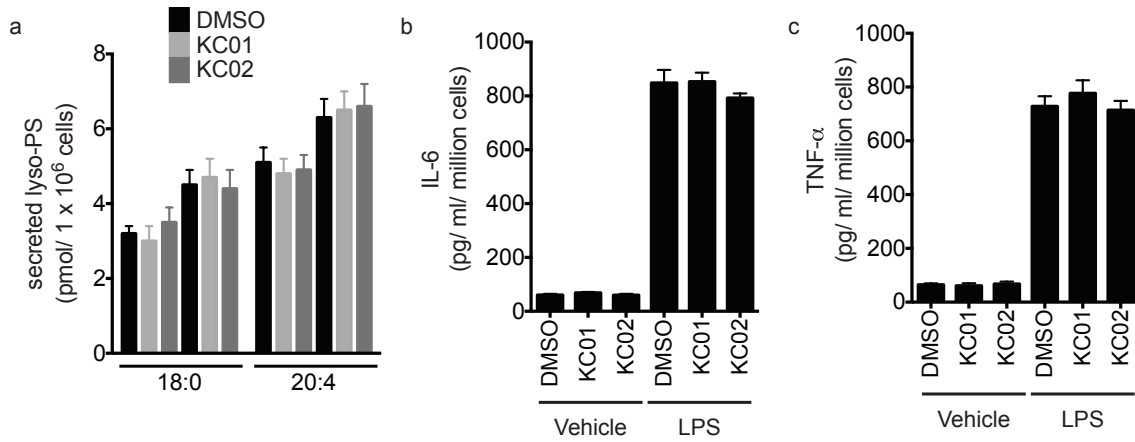
ABPP analysis of the membrane proteomes of spinal cord tissue from ABHD16A^{+/+}, ABHD16A^{+/-} and ABHD16A^{-/-} mice treated with (a) FP-rhodamine (2 μM, 30 min, 37 °C) or (b) WHP01 (0.5 μM, 30 min, 37 °C) confirms complete and selective loss of ABHD16A in spinal cord tissue from ABHD16A^{-/-} mice. (c) RT-PCR analysis of spinal cord tissue from ABHD16A^{+/+} and ABHD16A^{-/-} mice confirms the absence of ABHD16A mRNA in the ABHD16A^{-/-} spinal cords. (d) PS lipase activity of spinal cord membrane proteomes from ABHD16A^{+/+}, ABHD16A^{+/-} and ABHD16A^{-/-} mice measured using a C18:0/C18:2 PS substrate (100 μM) as described in **Supplementary Fig. 1**. Data represent mean ± s. e. m. N = 3 per group. Student's t-test: * p < 0.05, ** p < 0.005 versus ABHD16A^{+/+} groups (e) Concentrations of lyso-PS lipids from spinal cords of ABHD16A^{+/+}, ABHD16A^{+/-} and ABHD16A^{-/-} mice. Data represent mean ± s. e. m. N = 4 per group. Student's t-test: * p < 0.05, ** p < 0.005 for ABHD16A^{-/-} versus ABHD16A^{+/+} groups.



Supplementary Figure 30. Analysis of thioglycollate-elicited peritoneal macrophages from ABHD16A^{-/-} mice. (a) ABPP gel showing the loss of ABHD16A activity in the membrane fraction of macrophages from ABHD16A^{-/-} mice (vehicle and LPS treatment). Membrane lysates from macrophages of ABHD16A^{+/+} and ABHD16A^{-/-} mice were treated with FP-rhodamine (2 μM, 30 min, 37 °C) or WHP01 (0.5 μM, 30 min, 37 °C). Loss of ABHD16A was confirmed by WHP01, whereas FP-rhodamine could not resolve ABHD16A signals relative to other macrophage serine hydrolase activities. (b) PS lipase activity of peritoneal macrophages from ABHD16A^{+/+}, ABHD16A^{+/-}, and ABHD16A^{-/-} mice. Thioglycollate-elicited peritoneal macrophages were harvested from ABHD16A^{+/+}, ABHD16A^{+/-} and ABHD16A^{-/-} mice and treated with vehicle (PBS) or LPS (5 μg/mL) for 7 h. Macrophage membrane fractions were then isolated and analyzed for PS lipase activity using a C18:0/C18:2 PS substrate (100 μM) as described in **Supplementary Fig. 1**. Note that ABHD16A deletion caused a significant reduction in macrophage PS lipase activity, and LPS treatment induced a significant increase in PS lipase activity in ABHD16A^{+/+} and ABHD16A^{+/-}, but not ABHD16A^{-/-} macrophages. Data represent mean ± s. e. m. N = 3 per group. Student's t-test: * p < 0.05, ** p < 0.005 for LPS- versus PBS-treated groups and *** p < 0.001 for ABHD16A^{-/-} versus ABHD16A^{+/+} groups.



Supplementary Figure 31. Secreted cytokine profiles of peritoneal macrophages from ABHD16A^{-/-} mice. Concentration of secreted cytokines IL-6 (a) and IL-1β (b) from thioglycollate-elicited peritoneal mouse macrophages from ABHD16A^{+/+}, ^{+/-} and ^{-/-} mice treated with vehicle (PBS) or LPS (5 μg/mL) for 7 h. Data represent mean ± s. e. m. for four biological replicates. Student's t-test: ** p < 0.005, *** p < 0.0001 for ABHD16A^{-/-} versus ABHD16A^{+/+} groups.



Supplementary Figure 32. Effect of KC01 and KC02 on secreted lyso-PS and cytokines from ABHD16A^{-/-} macrophages. Concentrations of secreted lyso-PS (a) and cytokines IL-6 (b) and TNF-α (c) from thioglycollate-elicited peritoneal mouse macrophages from ABHD16A^{-/-} mice treated with inhibitor (KC01 or KC02, 1 μM, 4 h) followed by vehicle (PBS) or LPS (5 μg/mL) for 7 h. Data represent mean ± s. e. m. for four biological replicates. KC01 and KC02 did not alter lyso-PS or cytokine secretion. Other secreted and cellular lipids in ABHD16A^{-/-} macrophages were also unchanged by KC01 or KC02 treatment (**Supplementary Table 1**).

References

- 1 Camara, K., Kamat, S. S., Lasota, C. C., Cravatt, B. F. & Howell, A. R. Combining cross-metathesis and activity-based protein profiling: new beta-lactone motifs for targeting serine hydrolases. *Bioorg Med Chem Lett* (accepted) (2014).
- 2 Blankman, J. L., Long, J.Z., Trauger, S. A., Siuzdak, G. & Cravatt, B. F. ABHD12 controls brain lysophosphatidylserine pathways that are deregulated in a murine model of the neurodegenerative disease PHARC. *Proc Natl Acad Sci U S A* **110**, 1500-1505 (2013).
- 3 Blankman, J. L., Simon, G. S. & Cravatt, B. F. A Comprehensive Profile of Brain Enzymes that Hydrolyze the Endocannabinoid 2-Arachidonoylglycerol. *Chem. Biol.* **14**, 1347-1356 (2007).